Available online at www.sciencedirect.com
SCIENCE DIRECT®
Journal of Chromatography A, 984 (2003) 59–66
JOURNAL OF CHROMATOGRAPHY A
www.elsevier.com/locate/chroma

Ion trap tandem mass spectrometric identification of thiabendazole phototransformation products on titanium dioxide

Paola Calza*, Simone Baudino, Riccardo Aigotti, Claudio Baiocchi, Ezio Pelizzetti
Università di Torino, Dipartimento di Chimica Analitica, via P. Giuria 5, 10125 Torino, Italy

Received 25 July 2002; received in revised form 22 October 2002; accepted 5 November 2002

Abstract

The purpose of this study is to artificially produce degradation intermediates of thiabendazole, which could be reasonably similar to those really present in the environment. The formation of by-products from thiabendazole transformation has been evaluated by adopting irradiated titanium dioxide as a photocatalyst. Several species more hydrophilic than the thiabendazole have been identified and characterized by HPLC–multiple MS. A pattern of reactions accounting for the observed intermediates is proposed. Two different parallel pathways are operating (and through these pathways the transformation of the molecule proceeds) leading to several intermediate compounds. The main steps involved are: (1) the hydroxylation of the molecule on the aromatic ring with the formation of a species having $[M+H]^+$ 218; a further oxidation leads to the ring-opening and to the formation of aldehydic and alcoholic structures ($[M+H]^+$ 270, 268 and 152); and (2) the cleavage of a C–C bond and the formation of a species having $[M+H]^+$ 119.

Keywords: Photocatalysis; Catalysts; Thiabendazole; Titanium dioxide; Organosulfur compounds

1. Introduction

Thiabendazole is a fungicide widely used both in preserving several plants from diseases (i.e. rice, tobacco, sugar cane, tomato, fruit, etc.) [1–3] and in the treatment of hepatic infestation by Dicrocoelium and Fasciola in goats and sheep [4,5]; it has also found application as topical and systemic drug in therapeutic treatment of cutaneous larva migrans [6–8].

The persistence of pesticide residues in agricultural products destined to human consumption is one of the most important problems connected to their use. Several studies have been performed to search residues, for example in milk [9,10] and in fruit juice [11]. The presence of traces of thiabendazole has been also found in surface and ground waters [12,13]. Whatever the concentration level found, they have to be removed either to protect our water resources or to achieve drinking water quality. Developments in the field of chemical water treatment have made available several oxidative degradation procedures for pesticide elimination. Among them are particularly important the photochemical advanced oxidation processes (AOPs), such as TiO_2/UV or photo-Fenton reactions.

Chemical oxidation processes generate a great

*Corresponding author. Fax: +39-11-670-7615.
E-mail address: paola.calza@unito.it (P. Calza).

0021-9673/02/$ – see front matter
PII: S0021-9673(02)01837-X

number of by-products at quite low concentrations, which may well be considered the goal of the treatment but which render difficult their chemical analysis. In these conditions elucidation of the structures of degradation products is only possible by applying sophisticated analytical tools such as a GC or LC in combination with mass spectrometry. Thiabendazole can be detected only by adopting liquid chromatography [14]. The degradative processes do not necessarily bring a decrease in the toxicity and can lead to the formation of intermediates having an even increased toxicity and stability, as found for example in the degradation of chlorophenols that leads to biphenyls formation [15]. Then, it may be of interest to investigate the thiabendazole degradation and to identify its transformation products.

In the present study, the thiabendazole has been irradiated using titanium dioxide as a photocatalyst and the main transformation products have been identified and characterized through a multiple MS (MS^n) spectra analysis. Heterogeneous photocatalytic processes involve reactions at the surface–catalyst interface [16]. When irradiating with photons of energy equal to or exceeding the band gap energy of titanium dioxide (anatase, 3.2 eV band gap), valence band (VB) electrons are promoted to the conduction band (CB). Valence band holes [$E_0 = +3.1$ eV versus normal hydrogen electrode (NHE) at pH 0] and reductive conduction band electrons ($E_0 = -0.1$ eV) are generated:

$$TiO_2 + h\nu \rightarrow e^-_{CB} + h^+_{VB} \quad (1)$$

The photodecomposition of thiabendazole could thus be carried out either by oxidative species or conduction band electrons. The photogenerated electrons and holes can recombine giving a null process or they can migrate to the surface of the particle before recombination occurs. The photogenerated electrons could reduce the thiabendazole or react with the adsorbed molecular oxygen with superoxide radical anion $O_2\cdot^-$ formation. The photogenerated holes can directly oxidize the adsorbed thiabendazole or producing adsorbed OH radicals [17–19] through the surface bound OH^- or the adsorbed H_2O molecules.

2. Experimental

2.1. Material and reagents

All experiments were carried out using TiO_2 Degussa P25 as the photocatalyst. In order to avoid possible interference from ions adsorbed on the photocatalyst, the TiO_2 powder was irradiated and washed with distilled water until no signal due to chloride, sulfate or sodium ions could be detected by ion chromatography.

Thiabendazole (Aldrich) was used as received. HPLC grade water was obtained from MilliQ System Academie (Waters, Millipore). HPLC-grade methanol (BDH) was filtered through a 0.45-μm filter before use. Ammonium acetate reagent grade was purchased from Fluka (Sigma).

2.2. Irradiation procedures

The irradiation was performed using a 1500-W xenon lamp (Solarbox, CO. FO. MEGRA, Milan, Italy) simulating AM1 solar light and equipped with a 340-nm cut-off filter. The irradiation spectrum and the cells were identical to those described elsewhere [20]. The total photons flux (340–400 nm) in the cell and the temperature during irradiation has been kept constant for all experiments. They were 1.35×10^{-5} einstein min^{-1} and 50 °C, respectively. The irradiation was carried out on 5 ml of suspension containing 15 mg l^{-1} thiabendazole and 200 mg l^{-1} TiO_2. The entire content of the cells was filtered through a 0.45-μm filter and then analyzed by an HPLC–MS instrument.

2.3. Analytical procedures

2.3.1. Liquid chromatography

The chromatographic separations were run on a C_{18} Inertsil5 ODS3 column, 250×4.6 mm (Chrompack, The Netherlands). The injection volume was 100 μl and the flow-rate was 1.0 ml/min. An isocratic mobile phase composition was adopted: methanol–aqueous ammonium acetate 20 m*M* pH 6.8 (65/35).

2.3.2. Mass spectrometry

A LCQ MAT ion trap mass spectrometer (ThermoFinnigan) equipped with an atmospheric pressure interface and an atmospheric pressure chemical ionization (APCI) ion source was used. The LC column effluent was delivered into the ion source through a heated nebulizer probe (400 °C) using nitrogen as sheath and auxiliary gas (Claind Nitrogen Generator apparatus). The corona discharge voltage was set at the 5-kV value. The heated capillary value was maintained at 220 °C. The acquisition method used was previously optimized in the tuning sections for the parent compound (capillary, magnetic lenses and collimating octapoles voltages) in order to achieve the maximum of sensitivity. The tuning parameters adopted for APCI source were the following: Discharge current 5.00 μA, capillary voltage 3.00 V, capillary temperature 220 °C, tube lens −25 V; for ions optics, multipole 1 offset −3.00 V, electrostatic lens voltage −16.00 V, multipole 2 offset −7.00 V. Both electrospray ionization (ESI) and APCI ionization sources have been tested. Thiabendazole is stable with both ionization sources, thus, an APCI source has been adopted because it guarantees an higher sensitivity.

2.3.3. Carbon analyzer

Total organic carbon (TOC) and inorganic carbon (IC) were measured using a Shimadzu TOC-5000 analyzer (catalytic oxidation on Pt at 680 °C). Calibration was achieved by injecting standards of potassium phthalate.

3. Results and discussion

The concentration of thiabendazole (15 mg l^{-1}) has been chosen at the limit of its solubility in water to better identify the main by-products formed during the thiabendazole transformation. The disappearance of thiabendazole $[M+H]^+$ 202 is reported in Fig. 1, showing a pseudo first order kinetic and the total disappearance of the primary compound is achieved into 2 h. Concomitantly to the disappearance of $[M+H]^+$ 202, the formation of several peaks characterized by different m/z ratios is realized, as observable in the chromatographic profile reported in

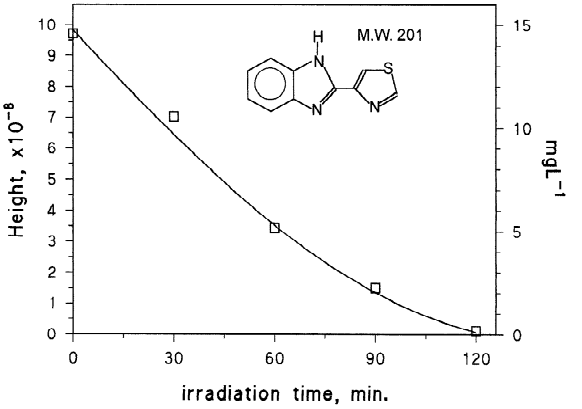

Fig. 1. Disappearance of thiabendazole (15 mg l^{-1}) on TiO_2 Degussa P25 200 mg l^{-1} as a function of irradiation time. Inset: thiabendazole [2-(1,3-triazol 4-yl) benzimidazole] molecular structure.

Fig. 2. The kinetics of formation and decomposition of the degradation intermediates need also to be determined in order to individualize the more stable intermediates. Fig. 3 shows typical bells shaped profiles of intermediates. On the basis of their chromatographic behavior and kinetics of evolution coupled with an accurate analysis of the MS and MS^n spectra the structures of the molecules reported on Fig. 4 are suggested.

As observable in Fig. 3, a further oxidation of the intermediates occurs; after 2 h of irradiation, all the identified intermediates have been degradated. It is well known that the photocatalytic process could provide the cleavage of the aromatic rings and, through the formation of aliphatic compounds, complete mineralization can be achieved [21–26]. For thiabendazole, the TOC results completely abated after 4 h of irradiation.

3.1. Thiabendazole MS^n study

Thiabendazole, whose molecular structure is reported in Fig. 1, has been characterised through an MS^n study. Confirmation of the molecular mass can be obtained by the MS spectrum which exhibited $[M+H]^+$ ion (m/z 202) as base peak (see Table 1). Several peculiar fragments were identified leading to a fragmentation pathway like the one proposed in

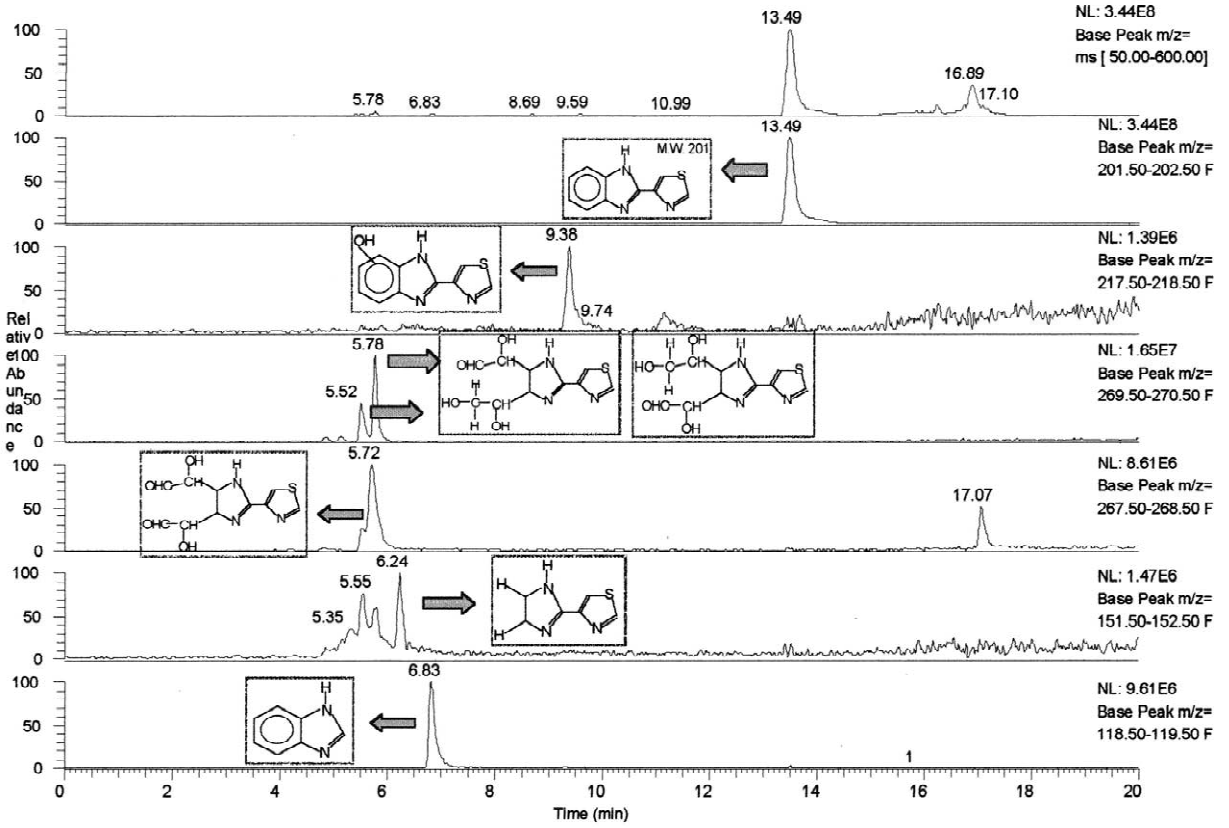

Fig. 2. Chromatographic profile of the solution at 60 min of degradation showing the species formed from the thiabendazole degradation; ions extracted from full scan chromatogram.

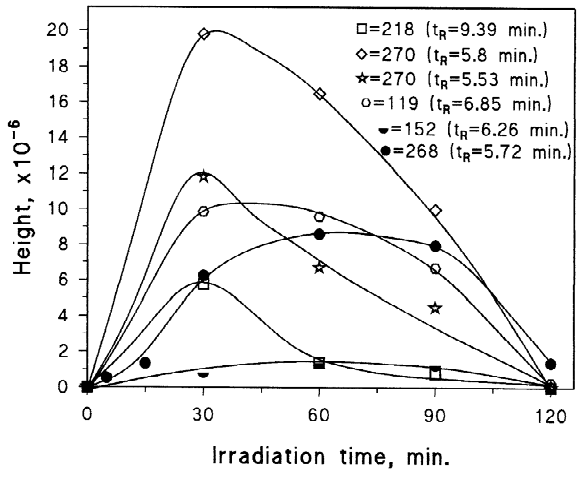

Fig. 3. Evolution of intermediates formed from the disappearance of thiabendazole (15 mg l^{-1}) degradation on TiO_2 200 mg l^{-1} as a function of irradiation time.

Fig. 5. MS^n could be applied using m/z 202 and 175 as precursor ions for MS^2 and MS^3 analysis, respectively. The fragment m/z 175, the only fragment observable in the MS–MS spectrum, is formed through a HCN loss; the fragmentation of this species leads to an MS^3 m/z value of 131.

Further fragments other than those shown in Fig. 5 have not been detected.

3.2. Intermediates MS^n study

Several intermediates were observed from the thiabendazole decomposition, as seen in the chromatographic profile obtained after 1 h of irradiation (see Fig. 2). An MS study, together with an MS^n study where it was possible, has been made. In several cases MS^n can be made and give more information, while unfortunately for some species

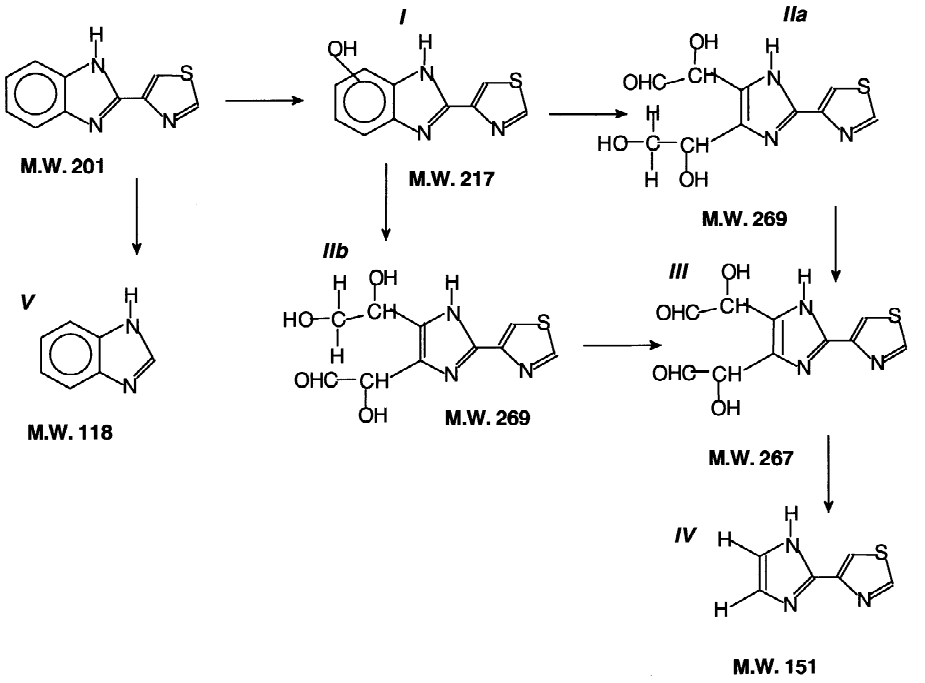

Fig. 4. Transformation pathways followed by thiabendazole. M.W., Molecular mass.

only information about the molecular mass and the presence of nitrogen and/or sulphur atoms can be extracted by the typical isotopic distribution. The overall fragments observed in the MS and MS^n spectra of the identified species, together with their retention times, are summarized in Table 1. The proposed structures are reported below.

3.2.1. Structure $[M+H]^+$ 218

This species comes from the hydroxylation of the thiabendazole molecule. The fragmentation is not particularly significant. Only the loss of a water molecule has been detected, indicating the presence of an alcoholic group not present in the initial species. This permits one to assign to this species the

Table 1
Main fragments coming from MS and MS^n spectra of the species represented in Fig. 4

$[M+H]^+$	t_R (min)	MS fragments, relative ions intensity	MS–MS fragments, relative ions intensity	MS^3 fragments relative ions intensity
202	13.5	202(100), 203(15), 158(3)	175(100), 176(15), 158(3)	175(30), 131(100), 143(25)
218	9.38	218(100), 219(10), 220(4)	200 (100), 201 (14)	–
152	6.24	152(100), 153(30), 126(18)	–	–
119	6.83	119 (100), 120 (8), 98(5)	–	–
270	5.52 5.78	270(100), 271(15), 268(30)	252(100), 234(15), 206(18)	234(100), 224(20), 206 (32), 196(4), 139(2)
268	5.72	268(100), 270(15)	250(100), 222(15), 208(10), 136(4)	250(16), 222 (100), 232(16), 205(6), 195(13), 161(1), 151(1)

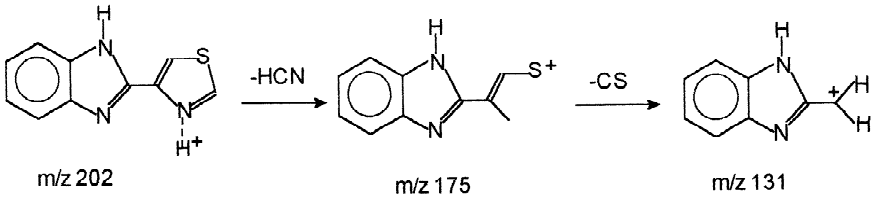

Fig. 5. Fragmentation pathway followed by thiabendazole.

structure of hydroxythiabendazole (see structure labelled I in Fig. 4), but the available information are not enough to determine in which position the OH radical attack occurs.

3.2.2. Structure [M+H]$^+$ 270

Two peaks, holding $[M+H]^+$ 270 and very similar retention times, were detected. The spectra of these species indicate that an odd number of nitrogen atoms and the sulphur atom are still present. Since the photocatalytic process could provide the cleavage of the aromatic rings, the $[M+H]^+$ 270 ions could be formed through a multiple OH radicals attach; the presence of several OH groups in the aromatic ring leads to the ring-opening. MS–MS and MS^3 spectra suggest that the two peaks follow the same fragmentation pathway. This could be in agreement with the proposed structures shown in Fig. 4 and labelled IIa and IIb. The fragments identified from the MS–MS and MS^3 spectra leads to the fragmentation pathway shown in Fig. 6 for the structure IIa (and similarly for the structure IIb). As seen in Fig. 6, the molecule $[M+H]^+$ lose a water molecule with the formation of m/z 252 (base peak in the MS^2 spectrum). This fragment leads to the formation of m/z 234 (loss of water) and m/z 206 (loss of CO). After that, the molecule is stable and no others significant fragments are observed. Using the $[M+H]^+$ 252 as precursor ion, the MS^3 is performed.

The MS^3 spectrum confirms that the favourite pathway is the one leading to m/z 234 (base peak in the MS^3).

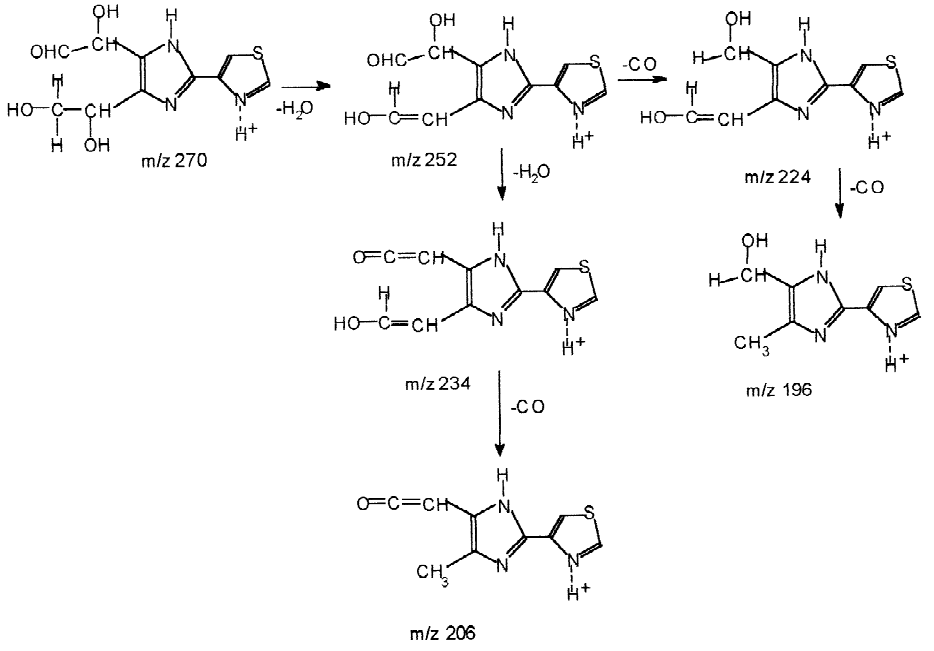

Fig. 6. Fragmentation pathway for the structure at $[M+H]^+$ 270.

Concomitantly, also the formation of m/z 224 (loss of CO) and m/z 196 (loss of CO) are observable as alternative (and secondary) pathway. The loss of two CO group (m/z 224 and 196) and of two water molecules (m/z 234 and 206) support the presence of three alcoholic groups and of a carbonylic group in the proposed structure for $[M+H]^+$ 270.

3.2.3. Structure $[M+H]^+$ 268

The oxidation of the alcoholic group contained in the species holding $[M+H]^+$ 270 leads to the formation of the molecule $[M+H]^+$ 268 (see structure labelled III in Fig. 4). This structure is supported by the MS^n spectra and follows the fragmentation pathway reported in Fig. 7.

The fragmentation pathway looks closely to the one followed by $[M+H]^+$ 270. The losses of two molecules of water (m/z 250 and 232) and of a CO group (m/z 222) confirm the presence of two alcoholic groups and of a carbonylic group.

3.2.4. Structure $[M+H]^+$ 152

The information extractable from the MS spectrum are: an odd number of nitrogen atoms is present, the sulphur atom is still present. Due to the low signal of this species, it was not possible to perform the MS–MS or MS^3 analysis. The proposed structure holding this molecular mass is labelled IV in Fig. 4. The formation of $[M+H]^+$ 152 is achieved through a sequence of oxidation occurring on the structure described above in Section 3.2.3 ($[M+H]^+$ 268).

3.2.5. Structure $[M+H]^+$ 119

Some information can be obtained from the MS spectrum of $[M+H]^+$ 119: an even number of nitrogen atoms are present, while the sulphur atom is absent as evidenced by the absence of the typical isotopic distribution. From such considerations we

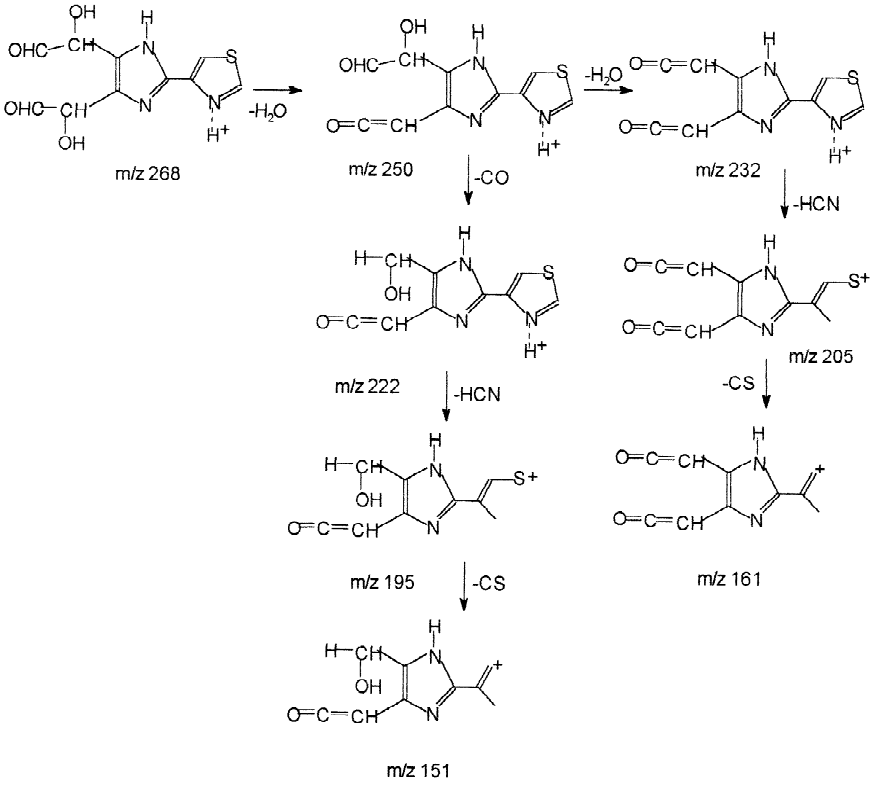

Fig. 7. Fragmentation pathway for the structure at $[M+H]^+$ 268.

have supposed a structure like the one labelled V (see Fig. 4).

This structure is formed through an OH radical attack on the C1′ and the consequent C–C chain broken. No fragments in MS^n were seen.

4. Conclusions

The ion trap mass spectrometry has been successfully applied to the determination of intermediate compounds resulting from the thiabendazole photo-assisted transformation, due to its ability to perform MS^n fragmentation. The proposed molecules are linked through two main pathways. The first one proceeds through a radical attack on the aromatic ring of the thiabendazole with the formation of the molecule having $[M+H]^+$ 218 (1-hydroxy-thiabendazole) and the consequent formation, through the ring opening, of the species $[M+H]^+$ 270, 268 and 152. The second pathway leads to the breaking of the molecule and the formation of the $[M+H]^+$ 119. Standards are not commercially available to confirm the identity of the proposed structures.

Future development will verify on real sample the identity of the proposed transformation products in order to confirm the feasibility of the proposed model to a contaminated environment.

References

[1] K. Bester, G. Bordin, A. Rodriguez, H. Schimmel, J. Pauwels, G. Van Vyncht, Fresenius J. Anal. Chem. 371 (2001) 550.
[2] X. Pous, M.J. Uiz, Y. Pico, G. Font, Fresenius J. Anal. Chem. 371 (2001) 182.
[3] A. Kaihara, K. Yoshii, Y. Tsumura, Y. Nakamura, Y. Ishimitsu Tonogai, J. Health Sci. 46 (5) (2000) 336.
[4] K. Ndamukong, M. Sewell, Vet. Parasitol. 41 (1992) 335.
[5] J. Durant, M. Toussaintgari, E. Bernard, P. Marty, Y. Lefichoux, P. Dellamonica, Sem. Hosp. Paris 67 (1991) 1507.
[6] G. Rizzitelli, G. Scarabelli, S. Veraldi, Int. J. Dermatol. 36 (1997) 700.
[7] K. Gougiotou, E. Nicolaidou, A. Panagiotopoulos, E. Hatziolou, A.D. Katsanihas, J. Eur. Acad. Dermatol. 15 (2001) 578.
[8] G. Albanese, C. Venturi, G. Galbiati, Int. J. Dermatol. 40 (2001) 67.
[9] A.L. Cinquina, A. Dilullo, F. Fiorucci, P. Calderini, R. Cozzani, Ind. Aliment. 34 (1995) 117.
[10] L. Prudhomme, F. Loche, P. Massip, Med. Mal. Infect. 32 (2002) 115.
[11] M.S. Young, M.F. Early, C.R. Mallet, J. Krol, J. AOAC Int. 84 (2001) 1608.
[12] S. Okita, Y. Ishii, S.J. Yun, Bunseki Kagaki 50 (2001) 127.
[13] L.E. Castillo, C. Ruepert, E. Solis, Environ. Toxicol. Chem. 19 (2000) 1942.
[14] M. Fernandez, Y. Pico, J. Manes, Chromatographia 54 (2001) 302.
[15] C. Minero, E. Pelizzetti, P. Pichat, M. Sega, M. Vincenti, Environ. Sci. Technol. 29 (1995) 2226.
[16] C. Minero, F. Catozzo, E. Pelizzetti, Langmuir 8 (1992) 481.
[17] C.S. Turchi, D.F. Ollis, J. Catal. 119 (1989) 483.
[18] D. Lawless, N. Serpone, D. Meisel, J. Phys. Chem. 95 (1991) 5166.
[19] G.K.C. Low, G.R. McEvoy, R.W. Matthews, Environ. Sci. Technol. 25 (1991) 460.
[20] C. Minero, E. Pelizzetti, S. Malato, J. Blanco, Chemosphere 26 (1993) 2103.
[21] R. Terzian, N. Serpone, C. Minero, E. Pelizzetti, J. Catal. 128 (1991) 352.
[22] E. Pelizzetti, C. Minero, V. Maurino, Adv. Colloid Interface Sci. 32 (1990) 271.
[23] W. Choi, M.R. Hoffmann, Environ. Sci. Technol. 29 (1995) 1646.
[24] E. Pelizzetti, C. Minero, Electrochim. Acta 38 (1993) 47.
[25] D.W. Bahnemann, J. Fox, E. Pelizzetti, P. Pichat, N. Serpone, in: G.R. Helz, R.G. Zepp, D.G. Crosby (Eds.), Aquatic and Surface Photochemistry, Lewis Publ, Boca Raton, FL, 1994, p. 261.
[26] M.R. Hoffmann, S.T. Martin, W. Choi, D.W. Bahnemann, Chem. Rev. 95 (1995) 69.